An Equilibrium Method for Continuous-Flow Cell Sorting Using Dielectrophoresis

M. D. Vahey and J. Voldman*

Department of Electrical Engineering and Computer Science, Massachusetts Institute of Technology, 77 Massachusetts Avenue, Building 36-824, Cambridge, Massachusetts 02139

Separations represent a fundamental unit operation in biology and biotechnology. Commensurate with their importance is the diversity of methods that have been developed for performing them. One important class of separations are equilibrium gradient methods, wherein a medium with some type of spatial nonuniformity is combined with a force field to focus particles to equilibrium positions related to those particles' intrinsic properties. A second class of techniques that is nonequilibrium exploits labels to sort particles based upon their extrinsic properties. While equilibrium techniques such as isoelectric focusing (IEF) have become instrumental within analytical chemistry and proteomics, cell separations predominantly rely upon the second, label-based class of techniques, exemplified by fluorescence-activated cell sorting (FACS) and magnetic-activated cell sorting (MACS). To extend the equilibrium techniques available for separating cells, we demonstrate the first implementation of a new microfluidic equilibrium separation method, which we call isodielectric separation (IDS), for sorting cells based upon electrically distinguishable phenotypes. IDS is analogous to isoelectric focusing, except instead of separating amphoteric molecules in a pH gradient using electrophoresis, we separate cells and particles in an electrical conductivity gradient using dielectrophoresis. IDS leverages many of the advantages of microfluidics and equilibrium gradient separation methods to create a device that is continuous-flow, capable of parallel separations of multiple (>2) subpopulations from a heterogeneous background, and label-free. We demonstrate the separation of polystyrene beads based upon surface conductance as well as sorting nonviable from viable cells of the budding yeast *Saccharomyces cerevisiae*.
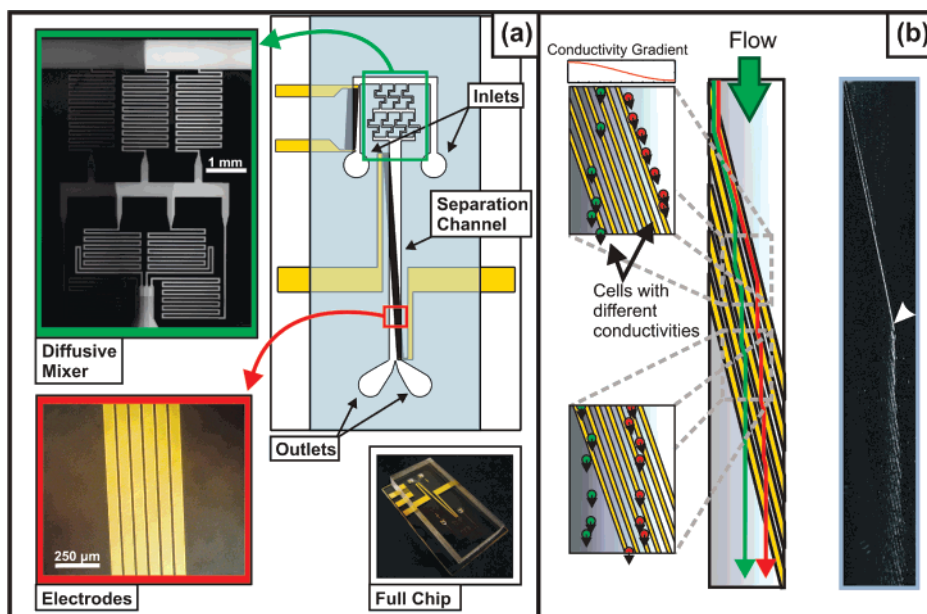
Cell separation typically relies upon *extrinsic* techniques (e.g., FACS), using labels to establish the specificity of the separation. While label-based methods benefit from the high specificity with which markers can be applied and detected, separating cells based upon *intrinsic* properties, where applicable, circumvents the time and cost associated with the design of new assays. Combining intrinsic separation with equilibrium gradient methods, where a force field applied in a spatially nonuniform medium focuses

particles to equilibrium positions, has revolutionized molecular separation over the past half century;[1−3] however, the relatively small niche in the context of cell sorting occupied by these methods reflects in part their limited variety (e.g., DGC, FFF) for effecting cell separation.[4,5] The utility of intrinsic equilibrium separations is directly related to the number of biophysical properties to which they can be applied. To extend their applicability to cell biology, we propose a new microfluidic equilibrium separation method, called isodielectric separation (IDS), that combines dielectrophoresis (DEP) with spatial gradients in electrical conductivity to sort electrically distinguishable cells and particles. While electrical methods have previously been used as the basis for cell separation, they have either been noncontinuous,[6] binary,[7] size-dependent,[8] and/or reliant upon counteracting forces to achieve separation,[5] thus limiting specificity. With IDS, we demonstrate the first true dielectrophoretic equilibrium gradient separation method, capable of performing continuous multiplex size-independent separation of cells.

IDS is analogous to isoelectric focusing (IEF), an equilibrium method where amphoteric molecules are forced via electrophoresis to the point in a pH gradient where their net charge vanishes, the isoelectric point. In IDS, the forcing mechanism is dielectrophoresis, directing cells to the point in a conductivity gradient where the net polarization charge vanishes, by analogy, the isodielectric point (IDP). Although it is possible to sort cells using IEF or other variations of electrophoresis,[9,10] in practice this is rarely done since surface charge provides a relatively nonspecific indicator of phenotype. Alternatively, because IDS separates particles based upon induced charge and is not limited to low-frequency electric fields, it may be used to probe both internal and external properties of living cells, giving access to a broader range of phenotypic markers.

---

* To whom correspondence should be addressed. E-mail: voldman@mit.edu. Fax: 617-258-5846.

(1) O'Farrell, P. H. *Science* **1985**, *227*, 1586−1589.
(2) Evans, L. L.; Burns, M. A. *Nat. Biotechnol.* **1995**, *13*, 46−52.
(3) Wang, Q. G.; Tolley, H. D.; LeFebre, D. A.; Lee, M. L. *Anal. Bioanal. Chem.* **2002**, *373*, 125−135.
(4) Brakke, M. K. *Methods Virol.* **1967**, *2*, 93−118.
(5) Huang, Y.; Wang, X.-B.; Becker, F. F.; Gascoyne, P. R. C. *Biophys. J.* **1997**, *73*, 1118−1129.
(6) Cummings, E. B.; Singh, A. K. *Anal. Chem.* **2003**, *75*, 4724−4731.
(7) Hu, X.; Bessette, P. H.; Qian, J.; Meinhart, C. D.; Daugherty, P. S.; Soh, H. T. *Proc. Natl. Acad. Sci. U.S.A.* **2005**, *102*, 15757−15761.
(8) Hawkins, B. G.; Smith, A. E.; Syed, Y. A.; Kirby, B. J. *Anal. Chem.* **2007**, *79*, 7291−7300.
(9) Ebersole, R. C.; McCormick, R. M. *Nat. Biotechnol.* **1993**, *11*, 1278−1282.
(10) Cabrera, C. R.; Yager, P. *Electrophoresis* **2001**, *22*, 355−362.

Figure 1. Device concept and architecture: (A) Layout of the device, consisting of two inlets, a diffusive mixer to establish the electrical conductivity gradient, and a separation channel, along which diagonal pairs of electrodes are arranged. (B) Operation of the device: cells are carried by flow to electrodes across the channel diagonal. The DEP force resolves with hydrodynamic drag to direct the particle across the width of the channel, in the direction of decreasing conductivity and thus toward the isodielectric point (IDP). To the right is a fluorescence micrograph of polystyrene beads deflected by the electrodes prior to reaching their IDP (arrow).

IDS represents a new microscale equilibrium separation method that separates cells based upon their intrinsic electrical properties under continuous flow. Each of these characteristics position IDS as an important complement to the existing battery of cell-sorting technologies. As we demonstrate, IDS enables the simultaneous, conductivity-specific resolution of complex mixtures, containing more than two types of particles, as well as separation of cells based upon differences in the electrical properties of those cells' membranes and cytoplasm.

Figure 1 illustrates the implementation of IDS described in this work. We create a monotonic gradient in electrical conductivity across the width of a microfluidic channel by injecting one solution of relatively high conductivity containing the cell mixture and a second solution of relatively low conductivity into a device with a diffusive mixer (Figure 1a, top left). This mixer generates a smooth monotonic conductivity profile that flows directly into a channel containing electrodes arranged across the diagonal (Figure 1a, bottom left). These electrodes guide the cells in the direction of decreasing medium conductivity, a one-sided approach to equilibrium, until the DEP force becomes sufficiently small that it is overwhelmed by hydrodynamic drag and the barrier is breached. The cells then continue downstream unobstructed for collection. Sampling cells from different portions along the channel width thus segregates cells according to their electrical properties. In that the separation occurs orthogonal to the axis of flow and is continuous, this implementation of IDS bears superficial similarity to other size-based DEP separation devices,[11] as well as other methods, such as those leveraging deterministic lateral displacement, magnetic, and acoustic forces to separate cells and particles

according to size and other properties.[12,13] Using IDS, we demonstrate the ability to simultaneously resolve three types of small (i.e., submicrometer radii) polystyrene beads according to their surface conductance, as well as yeast cells based upon membrane integrity.

THEORY

IDS requires that a medium with spatially varying electrical properties be combined with imposed electric fields and flow. The implementation of a DEP-based gradient separation method depends critically on controlling the nonlinear interactions that comprise this coupling and can potentially undermine the separation. While different considerations will arise depending upon the choice of implementation, in the following sections we restrict discussion to those issues specific to the particular implementation of IDS presented in this work.

Constraints from Transport and Force Balance. The IDS device must operate in a convection-dominated transport regime to ensure that the conductivity gradient is preserved over the channel length. This requirement is quantified by the dimensionless Péclet number (Pe $\equiv UL/D$, where U denotes the characteristic velocity of the fluid, L denotes the relevant length scale, and D is the diffusivity of the chemical species of interest) which increases with the significance of convection. The two length scales we are interested in are the channel width, w, from which the time scale for diffusion is obtained ($\sim w^2/D$), and the channel length, ℓ, which enters through the convective time constant ($\sim \ell/U$). This suggests that transport in the device is best parametrized in terms of the modified Péclet number, $w^2U/D\ell$, allowing us to

(11) Fiedler, S.; Shirley, S. G.; Schnelle, T.; Fuhr, G. *Anal. Chem.* **1998**, *70*, 1909−1915.

(12) Huang, L. R.; Cox, E. C.; Austin, R.; Sturm, J. C. *Science* **2004**, *304*, 987− 990.

(13) Pamme, N. *Lab Chip* **2007**, *7*, 1644−1659.

define for a given separation a critical number, Pe_0, below which that separation is no longer possible.

To study the relationship between transport (as parametrized by the Péclet number) and the range of electrical conductivities available for a separation further, we solve for the conductivity profile at the outlet of the device as a function of the Péclet number. To do this, we use a two-dimensional model for mass transport throughout the device; use of a two-dimensional model (rather than 3-D) is motivated by the rapid equilibration of the conductivity over the depth of the shallow channel. Solving the steady-state conservation equation for conductivity σ ($\mathbf{u}\cdot\nabla\sigma = \nabla^2\sigma$, where $\mathbf{u}$ is the fluid velocity vector) in dimensionless form gives

$$\tilde{\sigma} \equiv \frac{\sigma - \sigma_l}{\sigma_h - \sigma_l} = \frac{1}{2} + \sum_{n=1}^{\infty} a_n \cos(n\pi\tilde{x}) \exp(k_n\tilde{z}) \qquad (1)$$

Here, the x and z coordinates have been scaled according to the channel width and length, respectively (so that $\tilde{x} = x/w$ and $\tilde{z} = z/\ell$). The conductivity at the entrance of the device is bounded by high and low values of σ_h and σ_l, respectively. Defining the dimensionless groups $Pe = w^2 U/D\ell$ and $\gamma = \ell/w$ and assuming the conductivity at $z = 0$ (the entrance of the chamber) consists of M equally spaced levels ($M = 4$ in our architecture), we have $k_n = (^1/_2)(\gamma^2 Pe - [(\gamma^2 Pe)^2 + 4\gamma^2(n\pi)^2]^{1/2})$ and $a_n = \sum_{m=1}^{M-1} 2\{\sin(m(n\pi)/M)\}/\{(M-1)n\pi\}$. For cases in which $Pe \gg 2\pi\gamma^{-1}$, axial diffusion can be neglected and k_n simplifies to $k_n = -(n\pi)^2/Pe$. Combining this with eq 1 allows us to solve for the range of conductivities preserved along the separation channel as a function of Pe. Since the separation is based upon a mapping of the effective conductivity of a particle to the position along the channel width where it matches the solution conductivity, there is a direct correspondence between the range of conductivities preserved in the device and the maximum range of conductivities that can be simultaneously resolved. For example, if a sample contains particles varying in conductivity by a factor of 5, Pe must be maintained above ~18 to accommodate the full range, independent of other parameters and operating conditions.

The parameters that determine Pe also influence the forces throughout the system and in turn the maximum flow rate (and Pe) at which one can operate. Specifically, a particle will pass over the electrode barrier when the axial component of the drag and dielectrophoretic forces balance. This occurs when the real part of the complex Clausius−Mossotti factor, Re[CM] (a dimensionless measure of the dielectrophoretic mobility normalized to particle volume, which depends upon the medium conductivity), reaches a critical magnitude, |Re[CM_0]|, given by

$$|Re[\underline{CM}_0]| = f\frac{\mu \sin(\theta) h^2 U}{\epsilon_m a V_0^2} \approx f\frac{\mu D h^2}{\epsilon_m a V_0^2 w} Pe \qquad (2)$$

where μ denotes the fluid viscosity, θ ($\approx w/\ell$) denotes the angle of the electrodes with respect to the axis of the channel, h is the channel height, U is the mean fluid velocity, V_0 is the amplitude of the applied voltage, a is the particle radius, and ϵ_m is the permittivity of the fluid. The function f (≈ 250) is a dimensionless number that depends upon the geometric ratios within the system (e.g., channel height/electrode spacing). This expression is valid in the limit of dilute suspensions comprised of small particles ($a \ll h$) and in the absence of significant electrohydrodynamic flows, discussed shortly. Despite these restrictions, eq 2 offers some immediate insight into the specificity of the separation. For example, the minimum fractional change in Re[CM_0] that the device can resolve in the presence of particles of nonuniform size is roughly equal to the percent variation of particle size (ΔRe[CM_0]/Re[CM_0] = $\Delta a/a$). Thus for Re[CM_0] $\rightarrow$ 0 with particle size held constant, the specificity of the separation with respect to size variation improves, provided the assumptions inherent in eq 2 remain valid. Alternatively, this expression may be viewed as setting an upper bound on Pe; as the polydispersity (Δa) of the particles increases, higher specificity (and thus lower Pe) is required to resolve them.

Although the minimum Pe is related to transport and depends only upon the range of electrical properties present in the sample to be separated, the maximum Pe is constrained by force balance and can be increased through the channel geometry and operating voltage, as well as the physical properties of the solvent. To simultaneously satisfy the constraints imposed by force balance and transport, we design the separation channel to have a width of 1 mm, a length of 15 mm, and a height of $10-20~\mu m$. All of the experiments presented here were performed using an 18 μm high channel. The electrodes are arranged at an angle of 4° with respect to the channel axis, and the electrode gaps are 15 μm. With these parameters and a volumetric flow rate of 1 μL/min, the residence time in the separation channel is about 15 s, and the conductivity difference across the width of the channel is preserved to within ~78% of its original value over the entire length. Accordingly, the maximum ratio of conductivities (σ_h/σ_l) that we are able to maintain at the outlet of the device is $(1 + 0.78)/(1 - 0.78) \approx 8$, with the average conductivity being selected to suit the application. Doubling the flow rate increases the maximum conductivity ratio to ~20, with further improvements made possible by increasing the channel width.

Constraints from Electrohydrodynamic Flows. IDS is distinct from many other gradient separation methods in the extent to which the separation medium (the conductivity gradient) couples to the electric fields driving the separation. This coupling is bidirectional, as gradients in the properties of the medium can perturb the electric field, while the electric field can simultaneously perturb the medium, through both Joule heating and induced flow. While electrokinetics have been leveraged to mix and pump fluids at the microscale,[14,15] in the context of separations, they exert nonspecific forces that can undermine the ability to resolve different cells or particles. Although Pethig et al. demonstrated cell sorting in a *time-varying* conductivity,[16] we believe that the difficulties attendant to the strong coupling between electric fields and spatial variations in the fluid's electrical properties is why IDS has not previously been demonstrated.

We predict the electric field intensities we can use in the device by considering the influence of induced charge electroosmosis (ICEO) and electrohydrodynamics (EHD) driven by polarization

(14) Oddy, M. H.; Santiago, J. G.; Mikkelsen, J. C. *Anal. Chem.* **2001**, *73*, 5822−5832.
(15) Ajdari, A. *Appl. Phys. A: Mater. Sci. Process.* **2002**, *75*, 271−274.
(16) Pethig, R. *J. Biotechnol.* **1996**, *51*, 175−180.

of both the imposed conductivity gradient (intrinsic EHD) as well as gradients in conductivity and permittivity induced by Joule heating (thermal EHD). The strong frequency dependence of ICEO suggests that it will be negligible when the electrodes are driven in excess of ∼10 kHz.[17] For intrinsic and thermal EHD, we nondimensionalize the governing equations and solve numerically for the induced flow as a regular perturbation series (see Supporting Information). It follows immediately from scaling analysis that the DEP force and intrinsic EHD both scale proportional to E^2, while thermal EHD scales as E^4 (Supporting Information, Figure SI 1). Accordingly, at sufficiently low electric fields, thermal EHD will be subdominant to intrinsic EHD. The similar physics underlying intrinsic EHD and the DEP force on a particle, however, make decoupling these two phenomena by tuning the electric field intensity impossible. A simple scaling argument reveals that the relative magnitude of the DEP and induced drag forces is $\sim a^2 w/h^3$, where a is the particle radius and w and h are the channel width and height, respectively. This implies that the smallest particle that can be separated has a radius of the order $(h^3/w)^{1/2}$. Although this is shown by both numerical simulation and experiments to overpredict the minimum particle size by ∼3 times , it presents reasonable guidelines for sizing the device.

MATERIALS AND METHODS

Device Fabrication and Packaging. We pattern planar electrodes on 6 in. Pyrex wafers using e-beam evaporation of 2000 Å Au/100 Å Ti and a standard liftoff process. The electrode spacing and line width are 15 and 60 μm, respectively. For the microfluidic channels, we use PDMS replica molding from an SU-8 patterned silicon master (SU-8 2015, Microchem, Newton, MA) to create channels with a width of 1 mm and heights ranging from 10−20 μm, achieving ∼5% uniformity in film thickness over the area of the wafer. After dicing the glass wafer and manually drilling fluidic access holes, we plasma bond the PDMS channel to the chip. The PDMS channels are designed to be used once, mitigating any issues with fouling and contamination; for subsequent uses we strip the PDMS channel (Nanostrip 2X, Rockwood Electronic Materials, Derbyshire, U.K.) and bond a new channel in its place. We then affix the device to a custom printed circuit board, where we make the remainder of the electrical and fluidic connections.

Preparation of Cell and Bead Suspensions. We culture the budding yeast *Saccharomyces cerevisiae* at 30 °C for 2 days in a medium comprised of 1% yeast extract, 2% peptone, and 2% glucose. After harvesting the cells, we centrifuge and resuspend them in deionized water. We then transfer cells to be heat treated to a glass vial which we place on a hot plate set to 90 °C for ∼20 min. Live/dead staining using Syto 9 (S-34854, Invitrogen, Carlsbad, CA) and propidium iodide (P1304MP, Invitrogen, Carlsbad, CA) confirms that 100% of cells are nonviable after heat treatment, whereas typically >95% of the untreated cells remain viable. After staining, we wash the cells three times in a solution of deionized water, 0.1% BSA, and PBS mixed to the desired conductivity. For experiments involving polystyrene beads, we use three different types: blue fluorescent (17686-5, Polysciences, Inc., Warrington, PA, 1.6 ± 0.04 μm true diameter), red fluorescent (19508,

(17) Bazant, M. Z.; Squires, T. M. *Phys. Rev. Lett.* **2004**, *92*, 1−4.

Table 1. Crossover Frequency Measurements for Viable and Heat-Treated ("Nonviable") *S. cerevisiae*

medium conductivity [S/m]	viable frequency [kHz]	nonviable frequency [kHz]
0.0105	50 ± 10	25 ± 10
0.019	150 ± 25	100 ± 25
0.033	325 ± 25	−[a]
0.04	375 ± 25	−[a]
0.055	600 ± 50	−[a]

[a] The − denotes conditions under which no crossover was observed.

Polysciences, Inc., Warrington, PA, 1.755 ± 0.055 μm true diameter), and green fluorescent (FS04F/6845, Bangs Laboratories, Inc., Fishers, IN, 1.90 ± 0.22 μm true diameter).

Fluorescent Imaging, Data Acquisition, and Processing. We image the device using an upright Zeiss Axioplan 2M microscope (Zeiss, Thornwood, NY) coupled to a LaVision Imager 3 QE CCD digital camera (LaVision GmbH, Goettingen, Germany) using DAPI, FITC, and Cy3 filters. We record videos of particle separations under 5× magnification at the outlet of the device. To represent the trajectories of ensembles of particles over time in a 2D image, we process the videos using a first-order difference filter. We apply a uniform threshold, so that each particle receives identical weighting in the composite image and average the video over the total number of frames to produce the final image.

Electrical Characterization of Cells. To determine the optimal conditions (i.e., conductivity range and frequency) for separation, we measure the crossover frequencies of viable and nonviable *S. cerevisiae*. We stain cells for viability using Syto 9 (S-34854, Invitrogen, Carlsbad, CA) and propidium iodide (P1304MP, Invitrogen, Carlsbad, CA). By viewing cells under a triple band filter (61000v2, Chroma Technology Corp., Rockingham, VT), we are able to distinguish live and dead cells from one another simultaneously, enabling concurrent measurements under identical conditions. After staining, we wash the cells 3 times in solutions of deionized water doped to the desired conductivity using Dulbecco's phosphate buffered saline (Gibco, Carlsbad, CA). We then place the cell suspension in a sealed gasket above an array of interdigitated electrodes and vary the frequency until minimal response to the electric field is observed. We summarize the data in Table 1.

Electrical Characterization of Beads. We characterize the electrical properties of beads using the same technique as for cells. We wash and suspend the mixture of beads (diameters of 1.6, 1.75, and 1.9 μm) in a solution of known conductivity and search for the frequency at which the DEP force is minimized. We summarize the results from these measurements in Table 2.

Calculating the Separation Resolution. To estimate the degree to which we are able to separate viable from nonviable cells, we record videos of multiple separations immediately before the outlet of the device and obtain fluorescence intensity profiles, corresponding to the average distribution for ∼10^4 cells. From these fluorescence profiles, we obtain the separation resolution, R_s:

$$R_S = \frac{|X_1^{IDP} - X_2^{IDP}|}{2(\sigma_1 + \sigma_2)} \qquad (3)$$

Here, $X_{1,2}^{IDP}$ denotes the point around which the cells are centered, and $\sigma_{1,2}$ is the standard deviation of the distribution (not to be confused with electrical conductivity). By interpreting the fluorescence intensity plots as probability densities, $p_L(x)$ and $p_D(x)$, we determine the mean and standard deviations for the particle distributions using $\langle f(x) \rangle = \int f(x) p_{L,D}(x) \, dx$ with $X^{IDP} = \langle x \rangle$ and $\sigma = \langle x^2 \rangle - \langle x \rangle^2]^{1/2}$. Since striations in the distributions of cells created by the electrode gaps (where the concentration of cells is enhanced) cause the distributions to have considerable higher-order moments, we account for the non-Gaussian shape of the distributions by using an alternate interpretation of the standard deviation, integrating over the distribution and finding the width of the region over which the central most 68% of the cells are located.

Safety Considerations. Fabrication and cleaning of the devices involves toxic chemicals and is hazardous; these processes must be performed strictly in adherence with manufacturer guidelines in a ventilated environment. Additionally, cells should be treated as biohazards, with pathogenic strains maintained only in appropriate facilities.

RESULTS

Separation of Polystyrene Beads Based Upon Electrical Properties. We demonstrate the ability to resolve complex mixtures of micrometer-scale particles based upon differences in conductivity by using a mixture of three types of polystyrene beads in the device. Although bulk polystyrene is essentially dielectric, the effects of surface conductance can dominate for smaller beads, where the surface-to-volume ratio is greater.[18−20] This allows us to modulate the effective electrical properties of particles indirectly through size. Our characterization of the beads indicates that, for media conductivities less than ∼10 mS/m, crossover frequency varies inversely with size, supporting the hypothesis that the surface-to-volume ratio provides an avenue for modulating the electrical properties of the beads (Table 1). Importantly, although the complex interfacial phenomena that give rise to a particle's surface conductance are not fully understood, we observe that the DEP force on different particles vanishes at different combinations of frequency and medium conductivity. Thus, independent of the physical mechanism underlying their electrical properties, it should be possible to separate these particles using IDS.

We wash the beads in a medium with a conductivity of 9.1 mS/m and inject this and a low conductivity solution (comprised of deionized water) into the device. As we vary the frequency from 100 kHz to 10 MHz, the beads are resolved into three distinct flow streams, with the cleanest separation observed at 300 kHz (Figure 2a). Increasing the frequency further results in deflection to successively lower conductivities, until the DEP force becomes independent of the fluid and particle conductivities, culminating in the complete deflection of all particles across the channel at a

(18) Huang, J. P.; Karttunen, M.; Yu, K. W.; Dong, L. *Phys. Rev. E* **2003**, *67*, 7 pages.
(19) Maier, H. *Biophys. J.* **1997**, *73*, 1617−1626.
(20) Arnold, W. M. *J. Phys. Chem.* **1987**, *91*, 5093−5098.

Table 2. Crossover Frequency Measurements for Beads

medium conductivity [S/m]	1.60 μm beads frequency [kHz]	1.75 μm beads frequency [kHz]	1.90 μm beads frequency [kHz]
0.0033	180 ± 20	120 ± 20	40 ± 10
0.0063	120 ± 10	70 ± 10	40 ± 10
0.0092	100 ± 20	50 ± 10	−[a]
0.0121	80 ± 10	−[a]	−[a]

[a] The − denotes conditions under which no crossover was observed.

frequency of 10 MHz. We observe similar results in separations involving 1.25 μm beads (Figure 2c), which have a crossover frequency at the conductivity of interest of ∼5 MHz and thus separate into higher conductivity than the 1.6 μm blue beads in Figure 2a.

To confirm that the order of elution of the beads is based upon differences in their dielectrophoretic equilibrium rather than differences in particle size leading to different magnitudes of polarization, we repeat the assay with the solution conductivity held constant throughout the device (Figure 2b). In the uniformly conducting medium, we observe bistable behavior, with particles abruptly switching from zero to negative polarizability over a narrow frequency range (∼50−100 kHz). The necessity of a conductivity gradient in resolving these beads supports the conclusion that the separation is based upon differences in the equilibrium positions of the beads in a conductivity gradient rather than differences in bead volume and thus the magnitude of the DEP force. Additionally, the requirement for the conductivity gradient and the variation of the separation with frequency together preclude the possibility that the separation is due to any other nonelectrical parameter.

To further verify that the separation we observe is based upon surface conductivity as opposed to other properties that differ between the particles, we have performed complementary experiments in which we sort beads with comparable sizes but different surface coatings. For carboxyl-modified beads with comparable surface charge densities, differences in surface conductivity arise from differences in surface-to-volume ratio. Accordingly, smaller COOH-modified beads exhibit higher conductivities than larger, similarly functionalized beads and separate into higher conductivity solution, as illustrated in Figure 2. Alternatively, the absence of COOH surface modification should decrease the surface conductivity and hence the effective conductivity of the beads. This is exactly what is observed in Figure 3. Here small unmodified polystyrene beads exhibit lower effective conductivities than their larger and more highly charged counterparts (Figure 3). These experiments demonstrate that IDS may be used to separate particles according to their electrical properties, even in the presence of competing differences in the sizes of the particles.

Separation of Viable from Nonviable *S. cerevisiae*. A live/dead separation using *S. cerevisiae* demonstrates the feasibility of IDS for biological assays. To determine the appropriate conductivity range for the separation, we characterize viable and nonviable (heat treated) cells by measuring their crossover
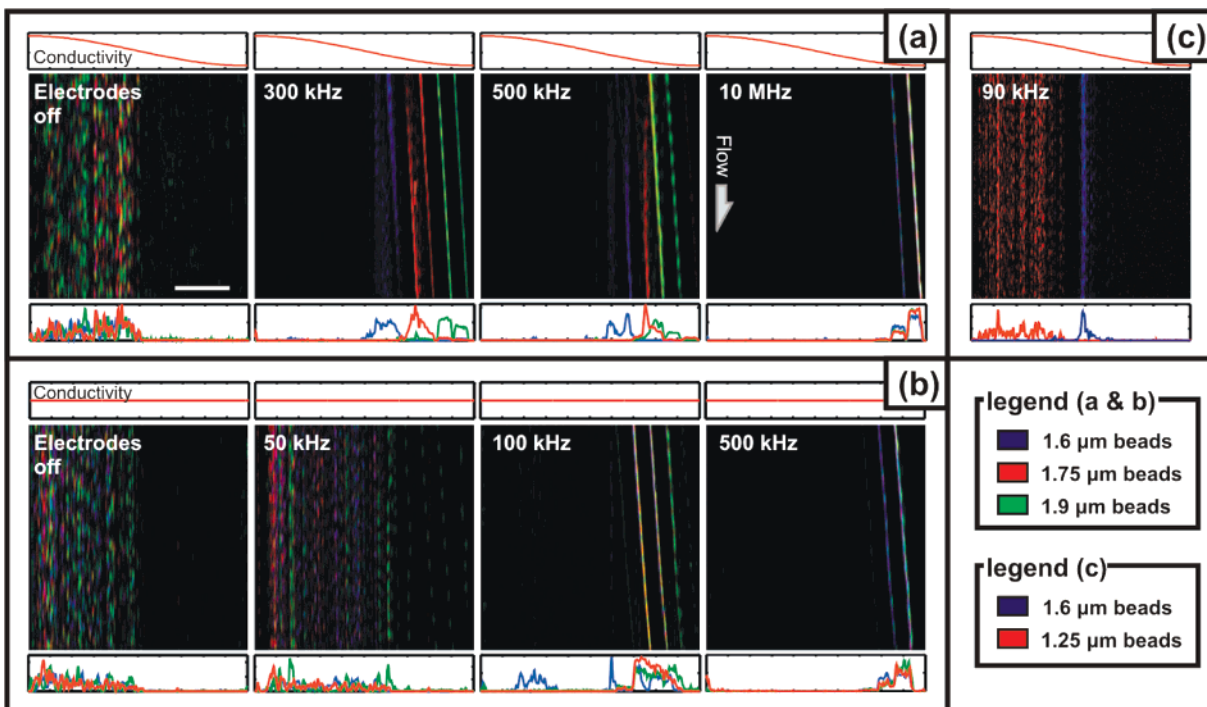
Figure 2. Simultaneous separation of three types of polystyrene beads based upon differences in surface conductance ($Q = 2~\mu$L/min, $V = 20~V_{pp}$). (A) In the presence of a conductivity gradient (ranging from 9.3 to $\sim$0 mS/m), we are able to cleanly resolve the three particle types simultaneously, with optimal separation occurring at $\sim$300 kHz. (B) In the absence of a conductivity gradient ($\sigma = 9.1$ mS/m), we observe bistability of the three particle streams, with transition from $|F_{DEP}| \sim 0$ to strong n-DEP over a narrow frequency band ($\sim$50 to $\sim$100 kHz). Note that the splitting of the blue particle stream at 100 kHz, apparent in the 1D cross section, is a consequence of the size dependence of the DEP force; however, no intermediate states are observed for any of the particles. (C) Further separation results obtained using polystyrene beads with different surface conductivities. Although the 1.25 μm beads (red) have positive polarizability at 90 kHz, the magnitude of this polarizability is sufficiently low to prevent accumulation of the beads on the electrodes.
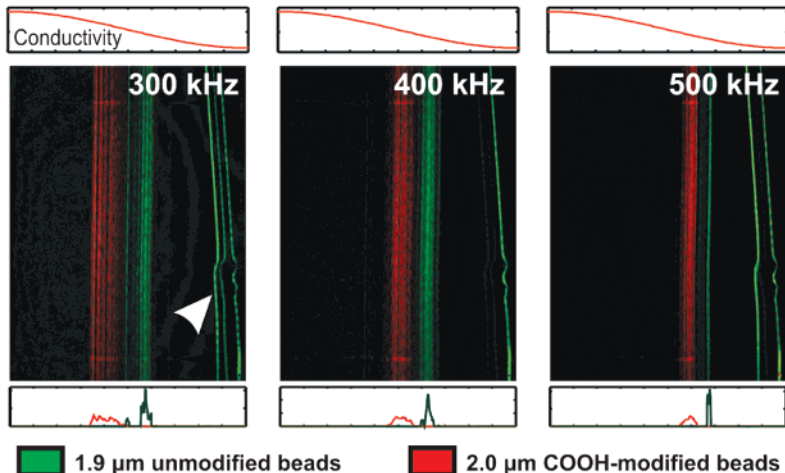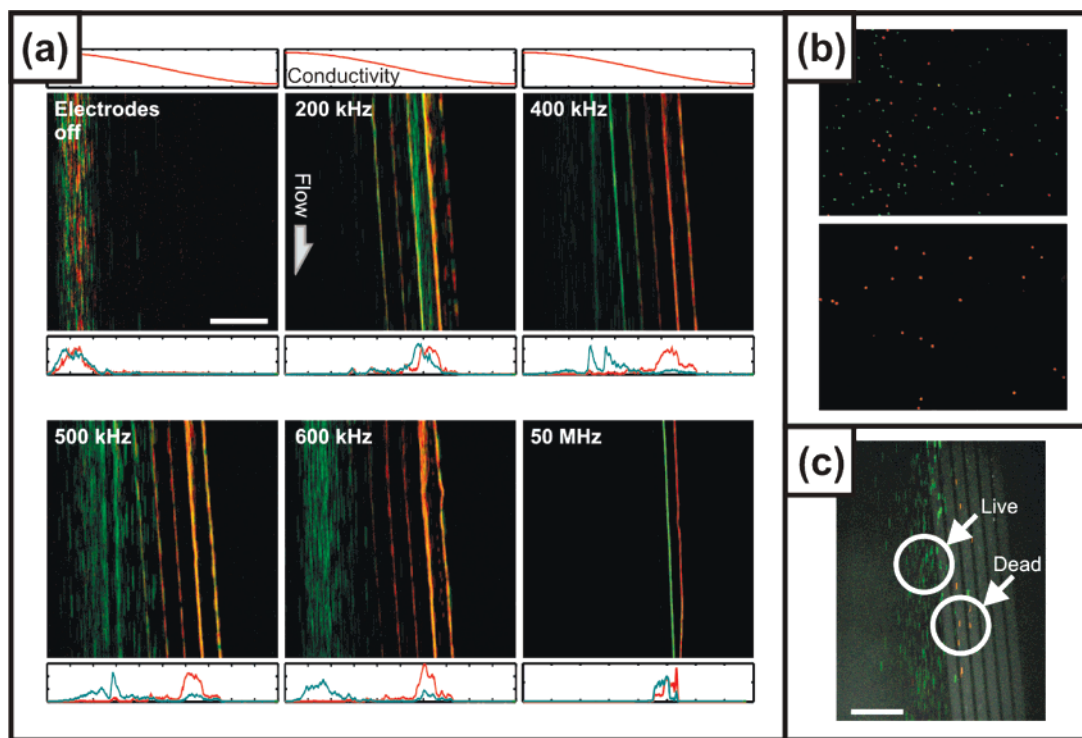

Figure 3. The separation of polystyrene beads based upon differences in surface conductivity, as determined by the presence or absence of modification with charged carboxyl (COOH) groups. Beads without carboxyl modification exhibit lower effective conductivities, despite competing differences in the surface-to-volume ratio. The arrow in the leftmost panel indicates particle aggregates which do not pass through the electrode barrier.

frequencies (Table 2). Consistent with previous observations,[21] we observe the homogenization of the DEP spectra of yeast cells upon heat treatment, a combined effect of increased membrane conductance and decreased cytoplasmic conductivity in nonviable versus viable cells. These measurements prescribe a conductivity that decreases from $\sim$50 to $\sim$10 mS/m across the channel and an applied frequency of $\sim$500 kHz.

(21) Huang, Y.; Hozel, R.; Pethig, R.; Wang, X. B. *Phys. Med. Biol.* **1992**, *37*, 1499−1517.

After the cells are stained and suspended in the higher conductivity fluid (40−50 mS/m), they are injected into the device along with the less conductive (10 mS/m) blank solution. Figure 4a depicts a sequence in which frequency is varied. Prior to the activation of the electrodes, both live and dead cells flow downstream uninhibited. Driving the electrodes at 200 kHz produces a deflection to lower conductivities for both live and dead cells. As we increase the frequency through $\sim$600 kHz, the electric field bypasses the membrane, probing the internal properties of

Figure 4. Live/dead separations of *S. cerevisiae*. (A) Frequency dependent behavior of live and dead cells in the device (σ_h = 47 mS/m, σ_l = 9.3 mS/m, Q = 3 μL/min, V = 20 V_{pp}). Optimal separation is observed at ∼600 kHz. (B) Collection of cells from high-conductivity (top) and low-conductivity (bottom) outlets, showing in particular the purity of collected nonviable cells (colored red). (C) Sorting nonviable cells directly from culture (i.e., without heat treatment).

the cell. Since viable cells retain the small ions that lend their cytoplasm its relatively high conductivity (∼0.2 S/m) while permeabilized cells do not, the effective conductivity of viable yeast increases with increasing frequency in this regime. Accordingly, we observe that the stream of live cells relax into the more conductive fluid as the frequency is increased. This trend continues until the effective conductivity of the cells exceeds that of the most conductive fluid in the channel (occurring at around 700 kHz for a maximum medium conductivity of 50 mS/m), and the cells undergo p-DEP upon reaching the electrode barrier. If the frequency is increased further still (>10 MHz), we exceed the inverse of the dielectric relaxation time associated with the polarization of the cytoplasm. In this limit, the DEP force becomes independent of the medium and particle conductivities, depending instead only on the relative permittivities. Because the fluid permittivity across the channel is essentially uniform and greater than the permittivities of both live and dead cells, the cells are unable to pass over the electrode barrier. Although heat treatment of yeast is known to reduce the cell size by ∼5−10%, our observations cannot be attributed to size dependence, since it is the nonviable cells that undergo the greatest deflection.

In further studies, we have confirmed the separations observed under flow by collecting cells and imaging the separated samples under a coverslip (Figure 4b). Also, we have observed that separation and enrichment of rare cells is not contingent on having comparable numbers of viable and nonviable cells, or on those cells being subjected to heat treatment protocol outlined previously. Specifically, we have achieved separation of live and dead yeast taken directly from culture, such that only a small percentage (<5%) are nonviable (Figure 4c).

We determined throughput and resolution for separations of viable and nonviable yeast by performing the assay at multiple flow rates using different cultures of cells in the same IDS device (Figure 5). At a frequency of 500 kHz and flow rates of 1.0 and 1.5 μL/min (for throughputs of 10^4 and 1.5×10^4 cells/min), we estimate the separation resolution (eq 3) to be 1.12 ± 0.15 and 1.25 ± 0.30, respectively. For separations performed in a frequency range over which the cells are purely conductive, this would correspond to a minimum resolvable difference in conductivity of ∼7.5 mS/m (corresponding to $R_s \approx 0.5$). The observation that a 50% increase in flow rate results in essentially no change in resolution suggests that the quality of the separation under these conditions is more strongly determined by intrinsic variability in the electrical properties of the cells than by nonspecific parameters, such as size (for which we measure these cells to have a coefficient of variation of 17%). We have additionally observed that the separation depends upon the concentration of cells injected into the device. While at 10^7 cells/mL, separation resolution falls to ∼0.6 ± 0.05 at a flow rate of 2 μL/min, decreasing the concentration to ∼0.5×10^6 cells/mL enables separation at flow rates up to 3 μL/min (Figure 4a, $R_s \sim 1.5$ at 600 kHz). This suggests that optimum throughput is achieved for high sample concentrations processed at moderately lower flow rates.

Besides resolution, a second metric for characterizing separations of complex mixtures is the peak capacity, which gives the maximum number of peaks that could be fit within the separation window.[22] Peak capacity is most commonly used to describe the performance of batch-mode separations, where the objective is

(22) Giddings, J. C. *Unified Separation Science*; John Wiley & Sons, Inc.: New York, 1991.
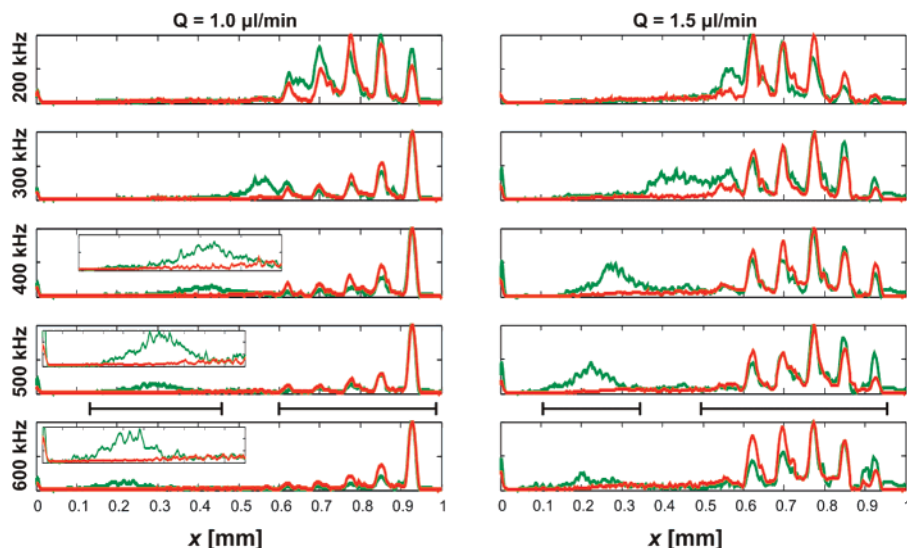
Figure 5. Representative fluorescence intensity cross sections showing distributions of viable (green) and nonviable (green and red) cells imaged at the outlet of the device. Bars at 500 kHz show ±2SD about the mean, as determined by integrating over the distribution.

to analyze the composition of the sample rather than sort it for collection. However, because IDS may be used as an analytic method as well as a preparative one, peak capacity serves as a relevant metric in evaluating the analytic potential of IDS. We estimate peak capacities of ~6 and ~4 for optimized separations of polystyrene beads and yeast, respectively. The increased predicted peak capacity for beads over yeast is not surprising, given that monodisperse, synthetic particles are likely to exhibit more narrowly distributed electrical properties than biological cells. Indeed, for applications in which the intrinsic variability of the particles' conductivities is very low, we would expect further improvement in peak capacity. We also note that, if the width of the particle distribution is limited by intrinsic conductivity differences, the peak capacity can be enhanced by using a larger range of conductivities, stabilized against diffusion and induced flow by adopting a correspondingly wider channel.

DISCUSSION

Equilibrium separations can be broadly defined as consisting of a medium with spatial nonuniformities combined with an imposed force field, giving rise to equilibrium positions to which particles stably converge. Within this common framework, however, exists considerable diversity. For example, the specificity of any equilibrium method is fundamentally connected to the nature of the equilibrium it is based upon; the number of intrinsic parameters to which the separation is sensitive will typically increase with the number of forces that combine to create the equilibrium. While the equilibrium position in DGC[4] is determined by, and thus specific to, density alone, DEP-FFF[5] relies upon the balance between counteracting gravitational and DEP forces and is therefore sensitive to both density and electrical properties. Accordingly, it is worth distinguishing between methods that achieve equilibrium through counteracting forces and those which exploit a single forcing mechanism that vanishes at some point in the medium, since the latter tend to offer greater specificity. Equilibrium methods may also be categorized according to such interrelated issues as whether they operate in

batch or continuous mode, whether they are micro- or macroscale, and the particular physics that they exploit. The equilibrium in IDS, the IDP, is established by a single forcing mechanism, and in the implementation we present here, particles are directed toward this equilibrium under continuous flow. Although the operation mode (batch or continuous) is not fundamentally constrained, IDS is inherently a microscale technology, as dictated by the strong dependence of DEP and fluid flow on the geometric scale.

Direct comparison of the resolution and peak capacity of IDS to similar parameters typical of equilibrium separations of biological molecules is complicated by the physically distinct mechanisms that limit performance in each case. While the resolution of molecular separations is fundamentally constrained by thermodynamics, the trajectories of individual particles in IDS are deterministic and directly measurable. Performance limits in IDS are thus largely determined by the intrinsic variability of the cells. Indeed, this feature of IDS could be leveraged as an analytical tool, capable of performing high-throughput measurements of distributions of electrical properties across large populations of cells. Despite these constraints, we are able to achieve $R_s > 1$ reproducibly over several months across several devices. Although the optimal conditions (e.g., frequency and flow rate) for a particular separation may vary from trial to trial, an initial calibration of the device prior to each separation can be performed to ensure optimal conditions. This is done by simply observing the separation under different conditions and choosing those that are most effective.

The new physical methodology we present, dielectrophoresis in the presence of nonuniform medium conductivity giving rise to particle-specific equilibrium positions, can be generalized to different architectures with different modes of operation. We envision IDS as a platform allowing researchers to proceed directly from the creation of a mutant library to screening for a target phenotype with a minimum of intermediate steps, since the separation is intrinsic and no labels are required. Simultaneously, IDS could be used as a quantitative tool; measuring the IDP of

particles as a function of frequency, for example, would provide an avenue for determining the impedance spectra for heterogeneous populations of cells, characterizing their electrical phenotype. Realizing these goals will be aided by full characterization of the device's performance, especially in the limits of small particle size and high average media conductivities. The role of higher-order effects, such as the electrostatic and hydrodynamic interactions between particles being sorted, must also be investigated further if IDS is to be extended into a fully quantitative analytic technique.[23] Although we have focused in this work on particles with sizes of ~1 μm, we expect that IDS can be scaled for separations of smaller or larger specimens (e.g., viruses and mammalian cells, respectively) with modifications to the size and architecture of the current device.

(23) Khusid, B.; Acrivos, A. *Phys. Rev. E* **1996**, *54*, 5428−5435.

SUPPORTING INFORMATION AVAILABLE

Additional information as noted in text. This material is available free of charge via the Internet at http://pubs.acs.org.